THE GERONTOLOGICAL SOCIETY OF AMERICA®

Journals of Gerontology: Biological Sciences
cite as: *J Gerontol A Biol Sci Med Sci*, 2022, Vol. 77, No. 3, 433–442
https://doi.org/10.1093/gerona/glab303
Advance Access publication November 1, 2021

OXFORD

Original Article

Role of mTOR in the Development of Asthma in Mice With Cigarette Smoke-Induced Cellular Senescence

Hyun Seung Lee, PhD[1] and Heung-Woo Park, MD, PhD[2,3,*]

[1]Biomedical Research Institute, Seoul National University Hospital, Seoul, Republic of Korea. [2]Department of Internal Medicine, Seoul National University Hospital, Seoul, Republic of Korea. [3]Department of Internal Medicine, Seoul National University College of Medicine, Seoul, Republic of Korea.

*Address correspondence to: Heung-Woo Park, MD, PhD, Department of Internal Medicine, Seoul National University College of Medicine, 03080 Seoul, Republic of Korea. E-mail: guinea71@snu.ac.kr

Received: March 24, 2021; Editorial Decision Date: September 29, 2021

Decision Editor: Rozalyn M. Anderson, PhD, FGSA

Abstract

The role of cellular senescence in the development of asthma is not well known. We aimed to evaluate the susceptibility of mice with cellular senescence to asthma development and determine whether the mTOR pathway played an important role in this process. Cellular senescence was induced in mice by intranasal instillation of 2% cigarette smoke extract (CSE). Subsequently, a low dose (0.1 μg) of house dust mite (HDM) allergens, which cause no inflammation and airway hyperresponsiveness (AHR) in mice without cellular senescence, was administered intranasally. To evaluate the role of the mTOR pathway in this model, rapamycin (TORC1 inhibitor) was injected intraperitoneally before CSE instillation. CSE significantly increased senescence-associated β-gal activity in lung homogenate and S100A8/9+ p-mTOR+ population in lung cells. Moreover, S100A8/9+ or HMGB1+ populations in airway epithelial cells with p-mTOR activity increased remarkably. Rapamycin attenuated all changes. Subsequent administration of low-dose HDM allergen induced murine asthma characterized by increased AHR, serum HDM-specific immunoglobulin E, and eosinophilic airway inflammation; these asthma characteristics disappeared after rapamycin injection. In vitro experiments showed significant activation of bone marrow-derived cells cocultured with S100A9 or HMGB1 overexpressing MLE-12 cells treated with HDM allergen, compared to those treated with HDM allergen only. CSE increased the levels of senescence markers (S100A8/9 and HMGB1) in airway epithelial cells, making the mice susceptible to asthma development due to low-dose HDM allergens by activating dendritic cells. Because rapamycin significantly attenuated asthma characteristics, the mTOR pathway may be important in this murine model.

Keywords: Animal model, Asthma, Cellular senescence, Cigarette smoking, HMGB1, mTOR protein, Sirolimus, S100A9

Cellular senescence, a cell fate toward irreversible replicative arrest, is a dynamic state characterized by metabolic shifts with increased glycolysis, decreased fatty acid oxidation, increased reactive oxygen species (ROS) generation, and acquisition of a senescence-associated secretory phenotype (SASP) (1). Chronological aging, chemotherapy and radiotherapy, supplemental oxygen, and cigarette smoke are associated with the accumulation of senescent cells (2–4). Cigarette smoke extract (CSE) induces cellular senescence in cultured primary alveolar epithelial type II cells, as evidenced by a dose- and time-dependent increase in senescence-associated β-galactosidase (SA-β-gal) activity and p21 (a cyclin-dependent kinase inhibitor) accumulation, which are known senescence markers (5). Moreover, CSE affects the reparative potential of lung fibroblasts by altering p53 and p21 expression and cell cycle progression to the S phase (6). Previous studies have shown that CSE-induced cellular senescence plays a role in the pathogenesis of chronic obstructive pulmonary disease (COPD) and idiopathic pulmonary fibrosis (7–9). Limited but distinct data have shown that cellular senescence is implicated in asthma pathogenesis. For example, in patients with asthma, bronchial fibroblasts demonstrate a higher proportion of SA-β-gal-positive staining, and p21 expression is elevated in the bronchial epithelium (10,11). However, little is known about the role of cellular senescence in the development of asthma.

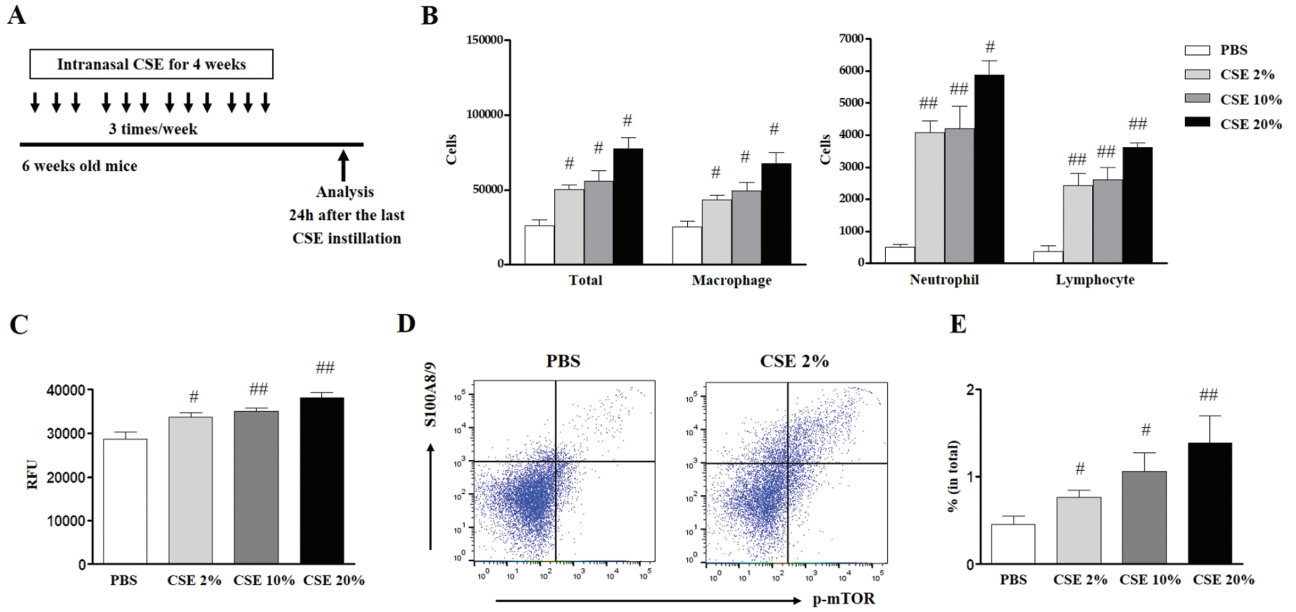

Figure 1. Effect of CSE on SA-β-gal activity and mTOR activation. (**A**) Experimental protocol (5–6 mice in each CSE group). (**B**) Inflammatory cells in bronchoalveolar lavage fluid. (**C**) SA-β-gal activity in lung homogenate. *Y* axis represents relative fluorescence unit (RFU). (**D**) Plot of S100A8/9+ p-mTOR+ population in lung cells. (**E**) The frequency of S100A8/9+ p-mTOR+ population in lung cells. *Y* axis represents the frequency of reading for total cells from lung cells. #$p < .05$, ##$p < .01$ compared to the control (PBS) group. PBS = phosphate-buffered saline; SA-β-gal = senescence-associated beta-galactosidase; CSE = cigarette smoke extract. Full color version is available within the online issue.

Mammalian target of rapamycin (mTOR), a large protein kinase belonging to the phosphatidylinositol 3 kinase-related kinase family, is the intracellular target of rapamycin (12). mTOR pathway is strongly associated with senescence in various cell types derived from humans or mice, and rapamycin reduces the expression of senescence markers in these cells (13,14). The role of the mTOR pathway in lung cell senescence has been extensively studied in COPD. Transgenic mice exhibiting mTOR overactivity in lung vascular cells or alveolar epithelial cells show cellular senescence and mimic COPD lung alterations (15). It has been reported that rapamycin, an inhibitor of TORC1, suppresses cigarette smoke-induced epithelial cell death and airway inflammation in COPD patients (16). However, to date, no study has evaluated the role of the mTOR pathway in the development of asthma due to cellular senescence.

In this study, we hypothesized that CSE-induced cellular senescence renders mice susceptible to allergic sensitization, resulting in the development of asthma, and the mTOR pathway plays an important role in the underlying processes. To test this, we first induced cellular senescence in murine lungs by intranasal instillations of CSE and then exposed the mice to low-dose house dust mite (HDM) allergens, which rarely cause airway inflammation or hyperresponsiveness in mice without cellular senescence. We examined whether this murine model developed cardinal features of asthma and further evaluated whether rapamycin treatment before CSE instillation attenuated these features.

Method

Preparation of CSE

Research-grade cigarettes (3R4F) were purchased from the Kentucky Tobacco Research and Development Center, The University of Kentucky (Lexington, KY). CSE was prepared following a previously described method (17). Briefly, one cigarette with its filter removed was fixed horizontally and burnt, and the main stream of smoke was aspirated at a constant flow rate (1 cigarette per 8 minutes) using a variable flow pump (CBS Scientific, San Diego, CA). Eight cigarettes were passed through 10 mL of a solvent to collect the CSE, and this content was defined as 100% (1 cigarette per 1 mL). This preparation was sterilized through a 0.22-μm syringe filter, and the prepared CSE was stored at −80°C until use.

Mouse Experiments

Six-week-old female BALB/C mice (18–20 g) were purchased from Orient Bio (Seoul, Korea). All experiments were performed with the approval of the Institutional Animal Care and Use Committee of the Institute of Laboratory Animal Resources at Seoul National University (SNU-200330-2) and Seoul National University Hospital (SNUH-IACUC 20-0248-S1A0). We used 2 study designs. In the first design, CSE (2%–20%) was suspended in phosphate-buffered saline (PBS), and rapamycin (25 mg; Santa Cruz Biotechnology, CA) was dissolved in dimethyl sulfoxide (1 mL; Sigma-Aldrich, MO); the stock of rapamycin (25 mg/mL) was suspended in PBS for administration to mice. Then, mice were instilled with CSE intranasally, and rapamycin (2 mg/kg) (18,19) was injected intraperitoneally at 30 minutes before CSE instillation (Figures 1A and 2A). In the second design, mice were administered with CSE or rapamycin for 4 weeks. After stopping CSE or rapamycin administration, mice were instilled intranasally with 0.1 μg HDM (*Dermatophagoides pteronyssinus*; Der p) allergen (Der p 1.88 μg/mg protein; Prolagen, Seoul, Korea) for 2 weeks (Figure 4A).

Measurement of SA-β-gal Activity in Lung Homogenate

Lung tissue (40 mg) from one of the lobes was homogenized in 0. 4 mL ice-cold cell lysis buffer containing protease inhibitor. The tissue homogenate was then incubated on ice for 30 minutes, and the lysates were centrifuged at 12 000 × *g* for 10 minutes at 4°C. The

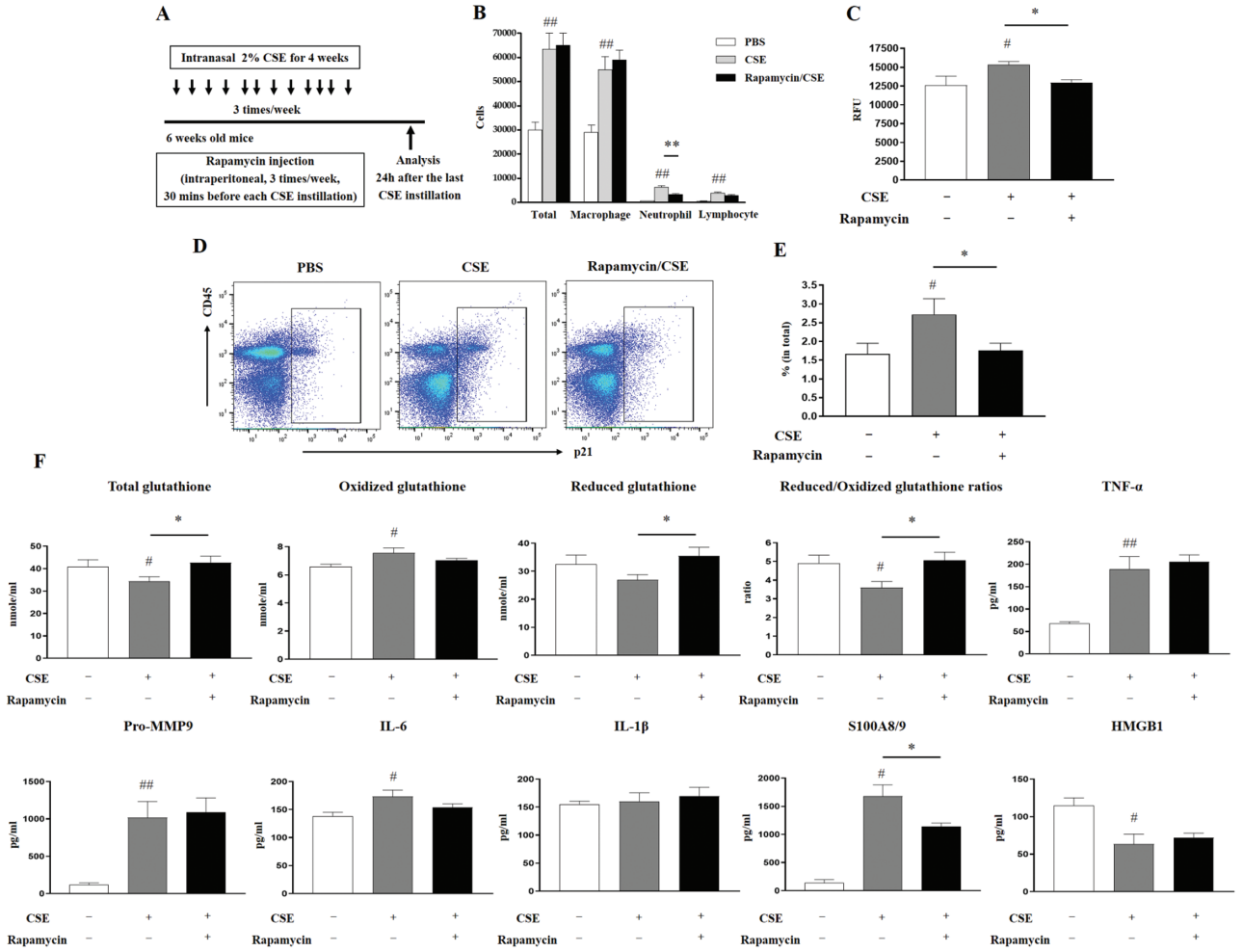

Figure 2. Effects of rapamycin on the CSE-induced changes of inflammatory and senescence-associated markers in lung and glutathione in serum. (**A**) Experimental protocol (5–6 mice in each group). (**B**) Inflammatory cells in bronchoalveolar lavage fluid. (**C**) SA-β-gal activity in lung homogenate. *Y* axis represents relative fluorescence unit (RFU). (**D**) A plot of p21+ population in lung cells. (**E**) The frequency of p21+ population in lung cells. (**F**) Total glutathione, oxidized glutathione and reduced glutathione levels, and reduced/oxidized glutathione ratios in serum were measured, and the detection time was 2 minutes. TNF-α, Pro-MMP9, IL-6, IL-1β, S100A8/9, and HMGB1 levels in bronchoalveolar lavage fluid were measured. #$p < .05$, ##$p < .01$ compared to control (PBS) group; *$p < .05$, **$p < .01$ between 2 groups. PBS = phosphate-buffered saline; SA-β-gal = senescence-associated beta-galactosidase; CSE = cigarette smoke extract. Full color version is available within the online issue.

supernatants were aliquoted and stored at −80°C. SA-β-gal activity (senescence-associated marker) was measured quantitatively using a cellular senescence activity assay kit (Enzo Life Sciences, NY). Fluorescence was measured using a Fluorescence Microplate Reader (Epoch Biotek, VT).

Measurement of Phospho-mTOR, p21, S100A8/9, and HMGB1 Expression Levels in Lung Cells

Flow cytometry analysis was used to measure phospho-mTOR (p-mTOR; activated mTOR), p21 (senescence-associated marker), S100A8/9, and HMGB1 (SASP-associated markers) expression levels in lung cells. Single cells prepared from lung tissue were analyzed by intracellular staining with FITC-conjugated anti-S100A8/9 antibody (Novus Biologicals, CO), PE/Cy7-conjugated anti-p-mTOR antibody (Thermo Fisher Scientific, MA), and APC-conjugated anti-p21 antibody (BD Biosciences, Santa Cruz, CA). For flow cytometry analysis, at least 1×10^5 cells were acquired using an LSR II (BD Biosciences). All data were analyzed using FlowJo ver. 10 software (BD Biosciences). To measure S100A8/9 and HMGB1 expression levels in various lung cells, single cells were first stained with PerCPCy5.5-conjugated anti-CD45 antibody, BV711-conjugated anti-CD4 antibody, BV506-conjugated anti-F4/80 antibody, APC/Cy7-conjugated anti-CD11c antibody, and BV421-conjugated anti-epithelial cell adhesion molecule (EpCAM) antibody, then with FITC-conjugated anti-S100A8/9 antibody and PE-conjugated anti-HMGB1 antibody (Thermo Fisher Scientific) for intracellular staining.

Measurement of Mediators in Bronchoalveolar Lavage Fluid and Serum

Tumor necrosis factor (TNF)-α (BioLegend, CA), Pro-MMP9 (R&D Systems, Abingdon, UK), interleukin(IL)-6 (BioLegend), IL-1β (BioLegend), S100A8/9 (R&D Systems), and HMGB1 (CUSABIO, Houston, TX) levels in bronchoalveolar lavage (BAL) fluid and Der p-specific immunoglobulin E (IgE) level in serum were measured using enzyme-linked immunosorbent assay according to the manufacturer's instructions. The concentrations of total, oxidized, and reduced glutathione in serum were calculated using a glutathione detection kit (Enzo Life Sciences).

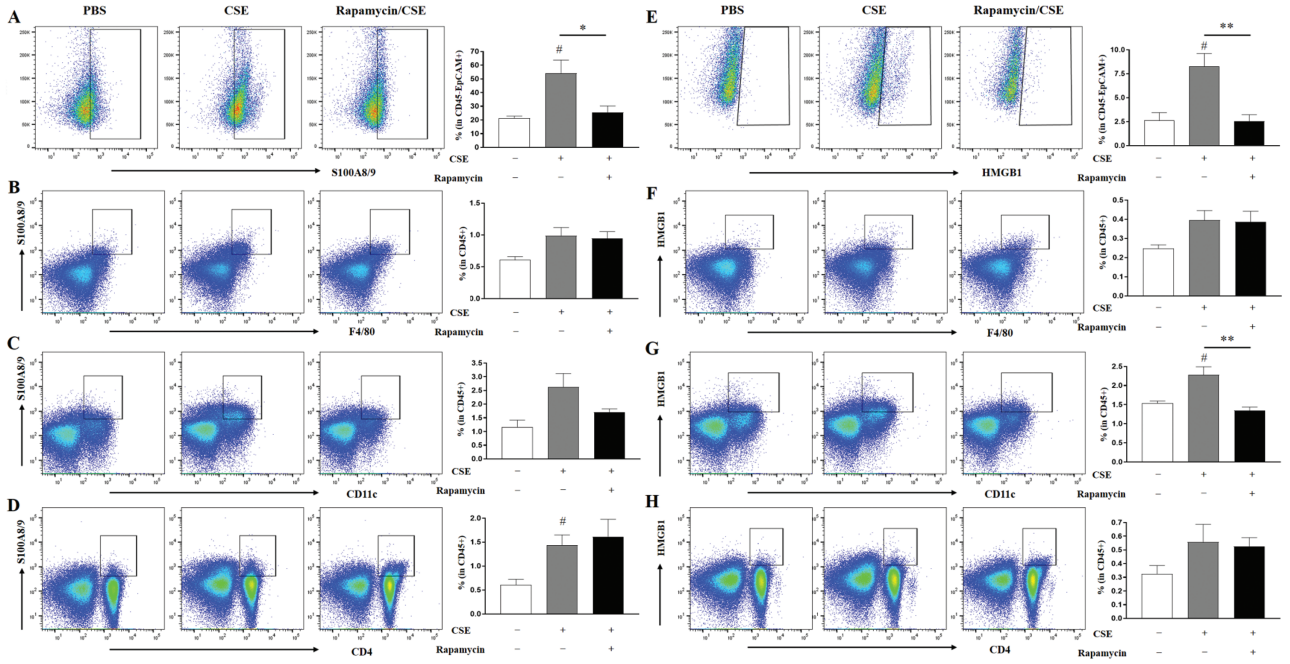

Figure 3. Effects of rapamycin on the CSE-induced changes of S100A8/9+ or HMGB1+ populations in various lung cells. (**A**) Gating plot and the frequency of S100A8/9+ population in CD45– EpCAM+ cells. (**B**) Gating plot and the frequency of S100A8/9+ F4/80+ population in CD45+ cells. (**C**) Gating plot and the frequency of S100A8/9+ CD11c+ population in CD45+ cells. (**D**) Gating plot and the frequency of S100A8/9+ population in CD4+ cells. (**E**) Gating plot and the frequency of HMGB1+ population in CD45– EpCAM+ cells. (**F**) Gating plot and the frequency of HMGB1+ F4/80+ population in CD45+ cells. (**G**) Gating plot and the frequency of HMGB1+ CD11c+ population in CD45+ cells. (**H**) Gating plot and frequency of HMGB1+ population in CD4+ cells. #$p < .05$ compared to control (PBS) group; *$p < .05$, **$p < .01$ between 2 groups. PBS = phosphate-buffered saline; CSE = cigarette smoke extract. Full color version is available within the online issue.

Airway Hyperresponsiveness

Dynamic resistance was measured using a Flexivent system (Scireq, Montreal, Canada). Mice were anesthetized with ketamine (90 mg/kg body weight) and xylazine (10 mg/kg body weight), tracheostomized, and connected to a flexivent ventilator via a 19-gauge cannula. Mice were ventilated using the following settings: tidal volume of 10 mL/kg body weight, 150 breaths/minute, and positive end-expiratory pressure 3 cm H_2O. Airway resistance (cm H_2O/mL/s) was measured using snapshot-150 perturbation. MCh (acetyl-b-methylcholine chloride; Sigma-Aldrich) provocation testing started with PBS, followed by MCh aerosols with increasing concentrations (0, 12.5, 25, and 50 mg/mL). The graphs show values of 25 and 50 mg/mL.

Histopathology

To evaluate and compare the severity and characteristics of pathological changes in the lung parenchyma, the left lungs of mice were fixed in 10% neutral buffered formalin and embedded in paraffin, and 3-mm sections were stained with hematoxylin and eosin (H&E).

Evaluation of Dendritic Cell Activation in Lung-Draining Lymph Node

Mice were sacrificed 24 hours after the last sensitization with Der p. The lung-draining lymph nodes were removed and processed. Single cells were stained with APC/cy7-conjugated anti-CD11c antibody (BD Biosciences), APC-conjugated anti-MHCII antibody, and PE-conjugated anti-CD86 antibody (Thermo Fisher Scientific). The proportion of dendritic cells (DCs) was determined by flow cytometry and defined as the fraction of MHCII+ or CD86+ in CD11c+ cells.

Measurements of Th Cells and S100A8/9 and HMGB1 Expression Levels in Lung Cells

Single cells prepared from lung tissue were stimulated with phorbol 12-myristate 13-acetate (100 ng/mL), ionomycin (1 μg/mL), and Golgi stop, then stained with PerCP-Cy5.5-conjugated anti-cluster of differentiation (CD) 45 antibody (Thermo Fisher Scientific). To quantify Th1, Th2, or Th17 cells, cells were stained with BV711-conjugated anti-CD4 antibody and PE-conjugated anti-IFN-γ, PE-Cy7-conjugated anti-IL-13, APC-conjugated anti-IL-5, or BV421-conjugated anti-IL-17A antibodies. To measure S100A8/9 and HMGB1 expression in various lung cells, single cells were stained with PerCP-Cy5.5-conjugated anti-CD45 antibody, BV711-conjugated anti-CD4 antibody, BV506-conjugated anti-F4/80 antibody, APC/Cy7-conjugated anti-CD11c antibody, and BV421-conjugated antiepithelial cell adhesion molecule (EpCAM) antibody, followed by intracellular staining with FITC-conjugated anti-S100A8/9 antibody and PE-conjugated anti-HMGB1 antibody (Thermo Fisher Scientific).

Effects of CSE With or Without Rapamycin on MLE-12 Cells

The effects of CSE, with or without rapamycin treatment, were assessed using a mouse lung epithelial cell line. Murine lung epithelial (MLE)-12 cells (SV40-transformed mouse-derived alveolar epithelial cell line; American Type Culture Collection, VA) were grown in Dulbecco's modified Eagle medium:Ham's F-12 containing 2% fetal bovine serum (FBS) in a humidified atmosphere at 37°C with 5% CO_2. The cells were then stimulated with CSE (2%) or rapamycin (2 nM) (20) for 24 hours. Intracellular ROS and SA-β-gal expression were detected using the oxidation-sensitive fluorescent probe dye

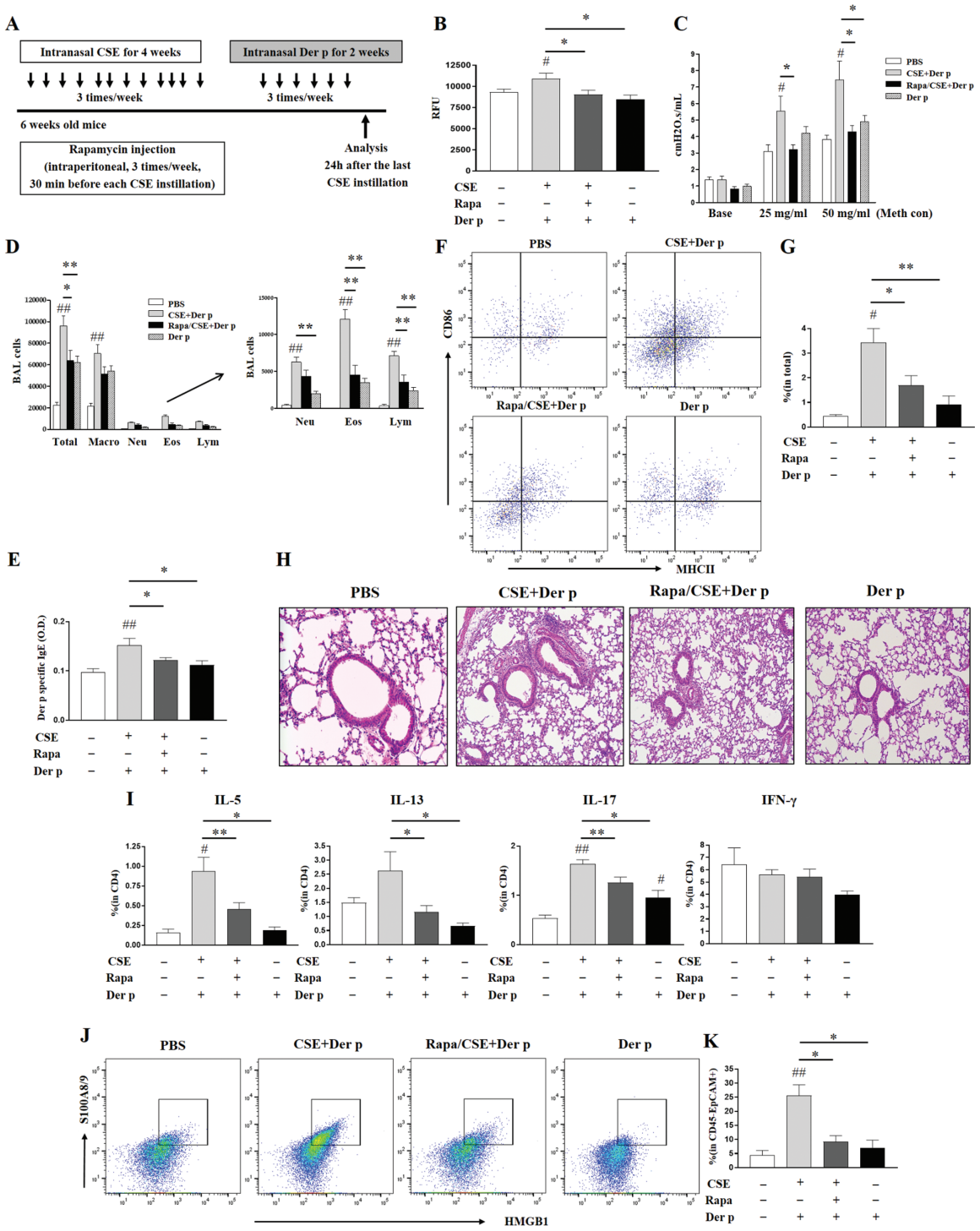

Figure 4. Murine asthma model with CSE-induced cellular senescence and effects of rapamycin on this model. (**A**) Experimental protocol (4–5 mice in each group). (**B**) SA-β-gal activity in lung homogenate. *Y* axis represents relative fluorescence unit (RFU). (**C**) Airway hyperresponsiveness. *Y* axis represents $cmH_2O.s/mL$. (**D**) Inflammatory cells in bronchoalveolar lavage fluid. (**E**) Serum *Der p*-specific IgE. *Y* axis represents OD (optimal density). (**F**) Gating plot of MHCII+ CD86+ population in CD11c+ cells from lung-draining lymph node. (**G**) The frequency of MHCII+ CD86+ population with CD11c+ in total cells from lung-draining lymph node. (**H**) Lung tissue (H&E stain, ×200). (**I**) The frequencies of IL-5+, IL-13+, IL-17+, and IFN-γ+ populations in CD4+ cells. (**J**) Gating plot of S100A8/9+ HMGB1+ population in CD45– Epcam+ cells. (**K**) The frequency of S100A8/9+ HMGB1+ population in CD45– Epcam+ cells. #$p < .05$, ##$p < .01$ compared to control (PBS) group; *$p < .05$, **$p < .01$ between 2 groups. Der p = *Dermatophagoides pteronyssinus*; Meth con = methacholine concentration; Macro = macrophage; Neu = neutrophil; Eos = eosinophil; Lym = lymphocyte; Rapa = rapamycin; CSE = cigarette smoke extract. Full color version is available within the online issue.

2′,7′-dichlorodihydrofluorescein diacetate (H2DCFDA; Invitrogen Molecular Probes, OR) and CellEvent Senescence Green Flow Cytometry Assay Kit (Invitrogen). Cells were incubated with 20 μM H2DCFDA or CellEvent Senescence Green Probe at 37°C for 30–60 minutes. The fluorescence due to DCF and SA-β-gal expression was detected using LSR II. To measure intracellular S100A8/9, HMGB1,

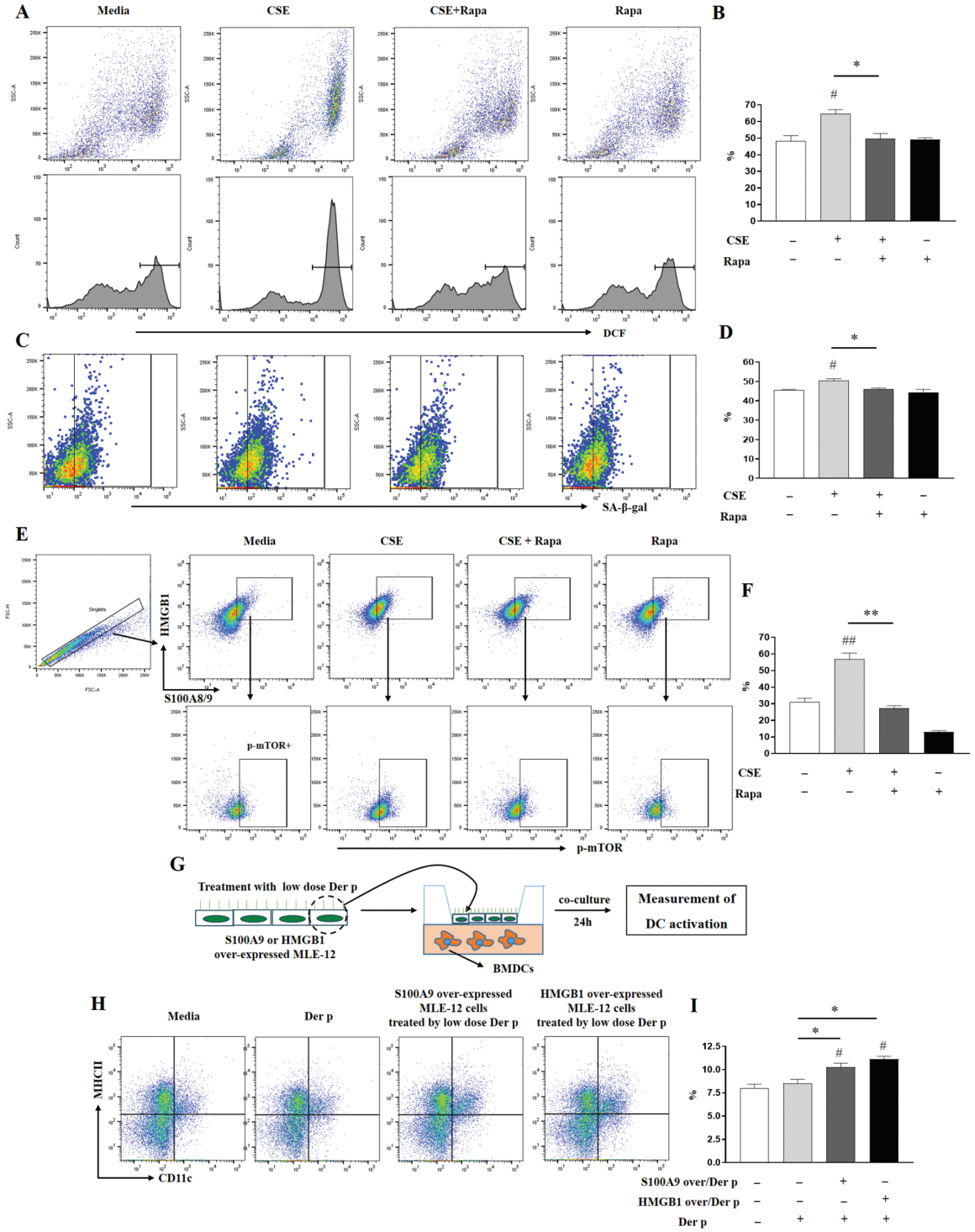

Figure 5. Effects of rapamycin on CSE-stimulated MLE-12 cells and effects of S100A9 or HMGB1 overexpressing MLE-12 cells treated by low-dose *Dermatophagoides pteronyssinus* allergen on dendritic cell activation. (**A**) Plot (upper) and histogram (lower) of DCF+ population in CSE-stimulated MLE-12 cells (with or without rapamycin). (**B**) The frequency of DCF+ population. *Y* axis of graph represents % of DCF+ cells. (**C**) Gating plot of SA-β-gal+ population in total cells from CSE-stimulated MLE-12 cells (with or without rapamycin). (**D**) The frequency of SA-β-gal+ population. (**E**) Gating plot of p-mTOR+ population in S100A8/9+ HMGB1+ cells in singlets from CSE-stimulated MLE-12 cells (with or without rapamycin). (**F**) The frequency of p-mTOR+ population in S100A8/9+HMGB1+ cells. (**G**) Experimental procedure. (**H**) Gating plot of MHCII+ CD11c+ population in BMDC after coculture with S100A9 or HMGB1 overexpressing MLE-12 cells. (**I**) The frequency of MHCII+ CD11c+ cells in BMDCs after coculture with S100A9 or HMGB1 overexpressing MLE-12 cells. #$p < .05$, ##$p < .01$ compared to media; *$p < .05$, **$p < .01$ between 2 groups. DCF = dichlorofluorescein; CSE = cigarette smoke extract. Full color version is available within the online issue.

and p-mTOR expression, single cells were stained with FITC-conjugated anti-S100A8/9 antibody, PE-conjugated anti-HMGB1 antibody, and PE/cy7-conjugated anti-p-mTOR antibody. The expression was also detected using LSR II.

Coculture of Bone Marrow-Derived Cells With S100A9 or HMGB1 Overexpressing MLE-12 Cells

To investigate the effect of S100A8/9 or HMGB1 on DC activation, bone marrow-derived cells (BMDCs) were prepared following the method described previously (21). At Day 7, BMDCs were seeded in the lower wells of Transwell inserts (pore size 0.4 μM; Costar). To perform S100A9 (a part of S100A8/9 heterodimer complex) or HMGB1 transfection, MLE-12 cells (2×10^5/well) were seeded in the upper wells of Transwell inserts and maintained overnight in Dulbecco's modified Eagle medium:Ham's F-12 with 2% FBS, then transfected with 0.2 μg of plasmid S100A9 or HMGB1 (*S100A9* or *HMGB1* Gene ORF cDNA clone expression plasmid; Sino Biological, Beijing, China) using Sinofection reagent (Sino Biological) according to the manufacturer's instructions. After washing, cells in the upper wells were treated with a low dose of Der p (10 μg/mL) and then placed in the lower wells with BMDCs. After 24 hours of coculture, cells were stained with APC/cy7-conjugated anti-CD11c antibody and APC-conjugated anti-MHCII antibody.

Statistical Analyses

Results are expressed as means ± standard deviation, and statistical differences among groups were assessed using the unpaired *t*-test and nonparametric Mann–Whitney *U* test. Statistical analyses were performed using GraphPad Prism (GraphPad Software, CA). *p* values less than .05 were considered significant.

Results

Effects of CSE on SA-β-gal Activity and mTOR Activation in Mouse Lung

Intranasal instillations of CSE significantly increased the populations of macrophages, neutrophils, and lymphocytes in BAL fluid and lung homogenate SA-β-gal activity in a dose-dependent manner (Figure 1A–C). Flow cytometry analysis showed that S100A8/9+ p-mTOR+ population in lung cells increased significantly in the same manner after CSE instillation ($p < .05$; Figure 1D and E). Based on these findings, 2% CSE (a minimum concentration causing changes) was used in subsequent experiments.

Effects of Rapamycin on CSE-Induced Changes in Mouse Lung

Intraperitoneal injections of rapamycin, administered 30 minutes before each CSE instillation (Figure 2A), significantly decreased neutrophil counts in BAL fluid and lung homogenate SA-β-gal activity ($p < .05$; Figure 2B and C). p21+ population in lung cells decreased significantly after rapamycin injections ($p < .05$; Figure 2D and E). We then assessed the effects of rapamycin on other changes induced by CSE, such as the expression of oxidative stress markers in serum and the pro-inflammatory cytokines S100A8/9 and HMGB1 in BAL fluid. Rapamycin reversed CSE-induced reductions in serum total glutathione levels and CSE-induced increases in serum oxidized glutathione levels (Figure 2F). In addition, rapamycin significantly increased reduced glutathione levels and reduced/oxidized glutathione ratios in serum, which had been reduced by CSE ($p < .05$; Figure 2F). Meanwhile, rapamycin showed no effects on CSE-induced increases in TNF-α, pro-MMP9, IL-6, and IL-1β levels in BAL fluid (Figure 2F). In terms of SASP-associated markers, rapamycin significantly reduced CSE-induced increases of S100A8/9 in BAL fluid ($p < .05$), but did not influence CSE-induced changes of HMGB1 in BAL fluid (secretory form; Figure 2F). To gain further insight, we measured intracellular levels of S100A8/9 and HMGB1 in cells with epithelial cell markers (CD45– EpCAM+), macrophage markers (CD45+ F4/80+), and DC markers (CD45+ CD11c+), as well as in CD4+ T cells using flow cytometry analysis of lung tissue. Populations of S100A8/9+ epithelial cells and T cells increased significantly after CSE instillation, but rapamycin significantly reduced the population with epithelial cell markers ($p < .05$; Figure 3A–D). Meanwhile, populations of HMGB1+ epithelial cells and DCs increased significantly after CSE instillation, and rapamycin significantly reduced both populations ($p < .05$; Figure 3E–H).

Murine Asthma Model With CSE-Induced Cellular Senescence and Effects of Rapamycin on This Model

We developed an asthma model by intranasally administering a low dose (0.1 μg/mouse) of Der p allergen to mice in which cellular senescence was induced by CSE (CSE + Der p group; Figure 4A). At the same time, we evaluated the effects of injecting rapamycin intraperitoneally 30 minutes before each CSE instillation (Rapa/CSE + Der p group) in this model. As expected, low-dose HDM allergen itself (Der p group) caused no differences in SA-β-gal activity, airway reactivity to methacholine, population of inflammatory cells in BAL fluid, and Der p-specific IgE level in serum compared to PBS (control group; Figure 4B–E). However, the CSE + Der p group showed significant increases in SA-β-gal activity ($p < .05$).

Airway hyperresponsiveness, neutrophil, eosinophil, and lymphocyte counts in BAL fluid, and Der p-specific IgE level in serum increased significantly in the CSE + Der p group compared to those in the control group ($p < .05$; Figure 4B–E). Interestingly, these increases were significantly attenuated in the Rapa/CSE + Der p group ($p < .05$; Figure 4B–E). In addition, MHCII+ CD86+ population in CD11c+ cells was significantly higher in the CSE + Der p group than in the control group, although rapamycin significantly decreased CSE-induced activation in CD11c+ cells (Rapa/CSE + Der p group; $p < .05$; Figure 4F and G). H&E staining revealed that inflammatory cells infiltrating airways in the Rapa/CSE + Der p group were lower than in the CSE + Der p group (Figure 4H). The populations of Th2 cells (IL-5+ or IL-13+ populations in CD4+ cells) and Th17 cells (IL-17+ population in CD4+ cells) increased significantly in the CSE + Der p group, but these increases were significantly attenuated in the Rapa/CSE + Der p group ($p < .05$; Figure 4I). In contrast, the population of Th1 cells (IFN-γ+ population in CD4+ cells) showed no differences among the groups (Figure 4I). S100A8/9+ HMGB1+ population in epithelial cells increased significantly in the CSE + Der p group compared to those in the control and Der p groups, and rapamycin significantly attenuated this increase (Rapa/CSE + Dp group; $p < .05$; Figure 4J and K).

Effects of Rapamycin on CSE-Stimulated MLE-12 Cells

CSE stimulated a significant increase in intracellular ROS level and SA-β-gal expression in MLE-12 cells, but rapamycin treatment

markedly reduced these (Figure 5A–D). Likewise, S100A8/9+ HMGB1+ population in MLE-12 cells increased significantly after CSE stimulation, but rapamycin significantly attenuated these increases ($p < .05$; Figure 5E). Moreover, this population showed increased expression of p-mTOR after CSE stimulation, which was significantly reduced after rapamycin treatment ($p < .05$; Figure 5E and F).

Effects of S100A9 or HMGB1 Overexpressing MLE-12 Cells Treated by Low-Dose Der p Allergen on DC Activation

To evaluate the roles of S100A8/9 and HMGB1, which exhibited increased expression levels in CSE-induced cellular senescence, we cocultured BMDCs with S100A9 or HMGB1 overexpressing MLE-12 cells treated with low-dose HDM allergen and assessed the activation markers of DCs (Figure 5G). As shown in Figure 5H and I, BMDCs cocultured with S100A9 or HMGB1 overexpressing MLE-12 cells treated with low-dose HDM allergen showed significantly increased levels of activation markers compared to those cultured with media or low-dose Der p allergen only ($p < .05$).

Discussion

Senescence-related changes are found in the lungs of asthmatics (10,11). In addition, thymic stromal lymphopoietin-induced cellular senescence is implicated in airway remodeling in asthma (22). However, in terms of cellular senescence, mechanistic links between environmental stimulants and asthma development have not been fully established, in contrast to COPD or idiopathic pulmonary fibrosis. In this study, we focused on the effects of cigarette smoke, a well-known inducer of cellular senescence, on asthma development (5). A recent meta-analysis showed that smokers have a high risk of developing sensitization to HDM allergens (23). In animal models, it has been reported that cigarette smoke induces allergic sensitization by promoting DC-mediated transport of allergens to lymph nodes or by temporarily disrupting normal lung homeostatic tolerance to innocuous inhaled allergens (24,25). However, previous studies were based on coexposures of cigarette smoke and HDM allergen and did not evaluate the possible role of cellular senescence induced by cigarette smoke prior to allergen exposure. Here, we induced cellular senescence in mouse lungs using CSE and found that mice with cellular senescence in lungs developed asthma features after subsequent exposure to low-dose HDM allergens, which alone does not cause airway inflammation and AHR in mice without cellular senescence. This murine model may more closely reflect asthma that onsets in adults and older people with cellular senescence induced by cigarette smoke, one of the major environmental stimulants.

Oxidative stress due to cigarette smoke activates the PI3K/AKT/mTOR signaling pathway, which accelerates lung aging when coupled with a reduction in sirtuin-1 activity (26,27). In line with previous reports, we observed that CSE instillations increased SA-β-gal activity and p-mTOR expression in lung cells as well as serum-reduced/oxidized glutathione ratios and that these changes were significantly attenuated by rapamycin. CSE instillations significantly increased serum levels of some SASP-associated markers, such as the inflammatory cytokines TNF-α, pro-MMP9, and IL-6, but rapamycin did not affect the expression of these cytokines. On the contrary, the SASP-associated markers S100A8/9 and HMGB1 (secretary form) in BAL fluid showed opposite changes after CSE instillation. Intracellular S100A8/9 and HMGB1 levels were significantly increased in epithelial cells after CSE instillation, and these increases were attenuated by rapamycin. Furthermore, we confirmed these changes by in vitro analysis using MLE-12 cell lines. A shift in the abundance of S100A8/9 is a distinctive feature of aging in mammalian tissues (28). HMGB1 protein depletion in senescent cell nuclei acts as an extracellular pro-inflammatory stimulus (29). S100A9 signaling contributes to the progression of age-related COPD, and HMGB1 has been reported to be a central mediator of senescence-associated inflammation (30,31). Damage-associated molecular patterns, including S100A8/9 and HMGB1, can stimulate the adaptive immune system by inducing maturation of DCs upon failure of tolerance mechanisms (32). Thus, damage-associated molecular patterns may play roles in the development of asthma by promoting allergic sensitization. Based on the previous observation that DCs are important to allergic sensitization (33), we focused on the changes in DCs induced by S100A8/9 or HMGB1, which exhibited increased expression in bronchial epithelial cells in our mouse model. Interestingly, DC activation markers were significantly increased in BMDCs cocultured with S100A9 or HMGB1 overexpressing bronchial epithelial cells. Our observations partly explain the sensitization by low-dose HDM allergens in mice with cellular senescence induced by prior exposure to CSE. Although it is known that airway epithelial senescence plays a pivotal role in the initiation of COPD (34), the results of this study provide the first evidence that airway epithelial cell senescence initiates the asthma onset through allergic sensitization.

In COPD, a causal relationship between lung cell senescence related to mTOR activation and emphysematous alterations has been suggested (15). Moreover, Zhang et al. (19) have reported that the activation of mTOR signaling is critical in the onset of asthma. Thus, mTOR signaling is important in the early stages of asthma development. In previous studies using a murine model, rapamycin administered during the induction (or sensitization) period significantly attenuated asthma features, but resulted in little or even aggravated airway inflammation when administered after sensitization (35,36). The single doses of HDM allergen used in these studies were 50 and 25 μg/mouse, which are much higher than that 0.1 μg/mouse dose used in this study. It has been reported that the HDM allergen itself causes DNA damage by inducing reactive oxygen and nitrogen species, thus potentially leading to cell death and senescence (37). Notably, DNA damage response is also involved in the mTOR signaling pathway (38). Although previous reports did not assess this possibility, the underlying mechanisms of HDM-induced cellular senescence, which differ from those of CSE-induced cellular senescence, may also be implicated in the pathogenesis of asthma. Taken together, cellular senescence induced by cigarette smoke, one of the major environmental stimulants, is critical in the development of asthma, and the mTOR signaling pathway plays an important role in this process. Further mechanism studies using cells with mutated mTOR (overexpression or knockout) will be necessary to confirm our observations.

In conclusion, we demonstrated that CSE-induced senescence increased S100A8/9 and HMGB1 expression in airway epithelial cells as well as DC activation, making mice susceptible to allergic sensitization and resulting in the development of asthma (graphical abstract, Supplementary Figure 1). In addition, we confirmed that the mTOR signaling pathway was important in this model by showing that rapamycin administration prior to CSE instillation significantly attenuated asthma features. To the best of our knowledge, this is the first study presenting evidence that cellular senescence induced by cigarette smoke, one of the major environmental stimulants, results in asthma susceptibility. The model used in this study will serve as a basis for understanding the onset of asthma in adult and older

populations. As discussed elsewhere, the mechanism of senescence is complex, involving different cell types and various signaling pathways (39). Thus, future studies on this model should focus on important cells or pathways other than airway epithelial cells and the mTOR pathway.

Supplementary Material

Supplementary data are available at *The Journals of Gerontology, Series A: Biological Sciences and Medical Sciences* online.

Funding

This work was supported by the National Research Foundation of Korea (NRF) grant funded by the Korea government (MSIT) (NRF-2019R1A2C1088473).

Conflict of Interest

None declared.

Author Contributions

H.S.L. and H.-W.P. designed the project, conducted experiments, analyzed the data, performed statistical analyses, and wrote the manuscript. All authors read and approved the final manuscript.

References

1. Kirkland JL, Tchkonia T. Cellular senescence: a translational perspective. *EBioMedicine*. 2017;21:21–28. doi:10.1016/j.ebiom.2017.04.013
2. Sabin RJ, Anderson RM. Cellular senescence—its role in cancer and the response to ionizing radiation. *Genome Integr*. 2011;2(1):7. doi:10.1186/2041-9414-2-7
3. Klimova TA, Bell EL, Shroff EH, et al. Hyperoxia-induced premature senescence requires p53 and pRb, but not mitochondrial matrix ROS. *FASEB J*. 2009;23(3):783–794. doi:10.1096/fj.08-114256
4. Ahmad T, Sundar IK, Lerner CA, et al. Impaired mitophagy leads to cigarette smoke stress-induced cellular senescence: implications for chronic obstructive pulmonary disease. *FASEB J*. 2015;29(7):2912–2929. doi:10.1096/fj.14-268276
5. Tsuji T, Aoshiba K, Nagai A. Cigarette smoke induces senescence in alveolar epithelial cells. *Am J Respir Cell Mol Biol*. 2004;31(6):643–649. doi:10.1165/rcmb.2003-0290OC
6. D'Anna C, Cigna D, Costanzo G, et al. Cigarette smoke alters cell cycle and induces inflammation in lung fibroblasts. *Life Sci*. 2015;126:10–18. doi:10.1016/j.lfs.2015.01.017
7. Araya J, Tsubouchi K, Sato N, et al. PRKN-regulated mitophagy and cellular senescence during COPD pathogenesis. *Autophagy*. 2019;15(3):510–526. doi:10.1080/15548627.2018.1532259
8. Gao N, Wang Y, Zheng CM, et al. β2-Microglobulin participates in development of lung emphysema by inducing lung epithelial cell senescence. *Am J Physiol Lung Cell Mol Physiol*. 2017;312(5):L669–L677. doi:10.1152/ajplung.00516.2016
9. Kanaji N, Basma H, Nelson A, et al. Fibroblasts that resist cigarette smoke-induced senescence acquire profibrotic phenotypes. *Am J Physiol Lung Cell Mol Physiol*. 2014;307(5):L364–L373. doi:10.1152/ajplung.00041.2014
10. Hadj Salem I, Dubé J, Boulet LP, Chakir J. Telomere shortening correlates with accelerated replicative senescence of bronchial fibroblasts in asthma. *Clin Exp Allergy*. 2015;45(11):1713–1715. doi:10.1111/cea.12611
11. Puddicombe SM, Torres-Lozano C, Richter A, et al. Increased expression of p21(waf) cyclin-dependent kinase inhibitor in asthmatic bronchial epithelium. *Am J Respir Cell Mol Biol*. 2003;28(1):61–68. doi:10.1165/rcmb.4715
12. Wullschleger S, Loewith R, Hall MN. TOR signaling in growth and metabolism. *Cell*. 2006;124(3):471–484. doi:10.1016/j.cell.2006.01.016
13. Demidenko ZN, Blagosklonny MV. Growth stimulation leads to cellular senescence when the cell cycle is blocked. *Cell Cycle*. 2008;7(21):3355–3361. doi:10.4161/cc.7.21.6919
14. Xu S, Cai Y, Wei Y. mTOR signaling from cellular senescence to organismal aging. *Aging Dis*. 2014;5(4):263–273. doi:10.14336/AD.2014.0500263
15. Houssaini A, Breau M, Kebe K, et al. mTOR pathway activation drives lung cell senescence and emphysema. *JCI Insight*. 2018;3:e93203. doi:10.1172/jci.insight.93203
16. Wang Y, Liu J, Zhou JS, et al. MTOR suppresses cigarette smoke-induced epithelial cell death and airway inflammation in chronic obstructive pulmonary disease. *J Immunol*. 2018;200(8):2571–2580. doi:10.4049/jimmunol.1701681
17. Lee HS, Park DE, Lee JW, et al. Critical role of interleukin-23 in development of asthma promoted by cigarette smoke. *J Mol Med (Berl)*. 2019;97(7):937–949. doi:10.1007/s00109-019-01768-y
18. Popovich IG, Anisimov VN, Zabezhinski MA, et al. Lifespan extension and cancer prevention in HER-2/neu transgenic mice treated with low intermittent doses of rapamycin. *Cancer Biol Ther*. 2014;15(5):586–592. doi:10.4161/cbt.28164
19. Zhang Y, Jing Y, Qiao J, et al. Activation of the mTOR signaling pathway is required for asthma onset. *Sci Rep*. 2017;7(1):4532. doi:10.1038/s41598-017-04826-y
20. Chen Y, Wang J, Cai J, Sternberg P. Altered mTOR signaling in senescent retinal pigment epithelium. *Invest Ophthalmol Vis Sci*. 2010;51(10):5314–5319. doi:10.1167/iovs.10-5280
21. Madaan A, Verma R, Singh AT, et al. A stepwise procedure for isolation of murine bone marrow and generation of dendritic cells. *J Biol Methods*. 2014;1:e1. doi:10.14440/jbm.2014.12
22. Wu J, Dong F, Wang RA, et al. Central role of cellular senescence in TSLP-induced airway remodeling in asthma. *PLoS One*. 2013;8(10):e77795. doi:10.1371/journal.pone.0077795
23. Mónico B, Gama JMR, Pastorinho MR, Lourenço O. Tobacco smoke as a risk factor for allergic sensitization in adults: conclusions of a systematic review and meta-analysis. *J Allergy Clin Immunol*. 2019;143(1):417–419. doi:10.1016/j.jaci.2018.07.040
24. Lanckacker EA, Tournoy KG, Hammad H, et al. Short cigarette smoke exposure facilitates sensitisation and asthma development in mice. *Eur Respir J*. 2013;41(5):1189–1199. doi:10.1183/09031936.00096612
25. Moerloose KB, Robays LJ, Maes T, Brusselle GG, Tournoy KG, Joos GF. Cigarette smoke exposure facilitates allergic sensitization in mice. *Respir Res*. 2006;7:49. doi:10.1186/1465-9921-7-49
26. Conti V, Corbi G, Manzo V, Pelaia G, Filippelli A, Vatrella A. Sirtuin 1 and aging theory for chronic obstructive pulmonary disease. *Anal Cell Pathol (Amst)*. 2015;2015:897327. doi:10.1155/2015/897327
27. Wang ZN, Su RN, Yang BY, et al. Potential role of cellular senescence in asthma. *Front Cell Dev Biol*. 2020;8:59. doi:10.3389/fcell.2020.00059
28. Wang S, Song R, Wang Z, Jing Z, Wang S, Ma J. S100A8/A9 in inflammation. *Front Immunol*. 2018;9:1298. doi:10.3389/fimmu.2018.01298
29. Davalos AR, Kawahara M, Malhotra GK, et al. p53-dependent release of Alarmin HMGB1 is a central mediator of senescent phenotypes. *J Cell Biol*. 2013;201(4):613–629. doi:10.1083/jcb.201206006
30. Railwah C, Lora A, Zahid K, et al. Cigarette smoke induction of S100A9 contributes to chronic obstructive pulmonary disease. *Am J Physiol Lung Cell Mol Physiol*. 2020;319(6):L1021–L1035. doi:10.1152/ajplung.00207.2020
31. Davalos AR, Kawahara M, Malhotra GK, et al. p53-dependent release of Alarmin HMGB1 is a central mediator of senescent phenotypes. *J Cell Biol*. 2013;201(4):613–629. doi:10.1083/jcb.201206006
32. Kono H, Rock KL. How dying cells alert the immune system to danger. *Nat Rev Immunol*. 2008;8(4):279–289. doi:10.1038/nri2215
33. Plantinga M, Guilliams M, Vanheerswynghels M, et al. Conventional and monocyte-derived CD11b(+) dendritic cells initiate and maintain T helper 2 cell-mediated immunity to house dust mite allergen. *Immunity*. 2013;38(2):322–335. doi:10.1016/j.immuni.2012.10.016

34. Antony VB, Thannickal VJ. Cellular senescence in chronic obstructive pulmonary disease: multifaceted and multifunctional. *Am J Respir Cell Mol Biol*. 2018;59(2):135–136. doi:10.1165/rcmb.2018-0061ED
35. Mushaben EM, Kramer EL, Brandt EB, Khurana Hershey GK, Le Cras TD. Rapamycin attenuates airway hyperreactivity, goblet cells, and IgE in experimental allergic asthma. *J Immunol*. 2011;187(11):5756–5763. doi:10.4049/jimmunol.1102133
36. Fredriksson K, Fielhaber JA, Lam JK, et al. Paradoxical effects of rapamycin on experimental house dust mite-induced asthma. *PLoS One*. 2012;7(5):e33984. doi:10.1371/journal.pone.0033984
37. Chan TK, Loh XY, Peh HY, et al. House dust mite-induced asthma causes oxidative damage and DNA double-strand breaks in the lungs. *J Allergy Clin Immunol*. 2016;138(1):84–96.e1. doi:10.1016/j.jaci.2016.02.017
38. Ma Y, Vassetzky Y, Dokudovskaya S. mTORC1 pathway in DNA damage response. *Biochim Biophys Acta Mol Cell Res*. 2018;1865(9):1293–1311. doi:10.1016/j.bbamcr.2018.06.011
39. Parikh P, Wicher S, Khandalavala K, Pabelick CM, Britt RD Jr, Prakash YS. Cellular senescence in the lung across the age spectrum. *Am J Physiol Lung Cell Mol Physiol*. 2019;316(5):L826–L842. doi:10.1152/ajplung.00424.2018